

Scalable Semi-supervised Learning with Graph-based Kernel Machine

Trung Le · Khanh Nguyen · Van Nguyen · Vu Nguyen · Dinh Phung

Received: date / Accepted: date

Abstract Acquiring labels are often costly, whereas unlabeled data are usually easy to obtain in modern machine learning applications. Semi-supervised learning provides a principled machine learning framework to address such situations, and has been applied successfully in many real-world applications and industries. Nonetheless, most of existing semi-supervised learning methods encounter two serious limitations when applied to modern and large-scale datasets: computational burden and memory usage demand. To this end, we present in this paper the *Graph-based semi-supervised Kernel Machine* (GKM), a method that leverages the generalization ability of kernel-based method with the geometrical and distributive information formulated through a spectral graph induced from data for semi-supervised learning purpose. Our proposed GKM can be solved directly in the primal form using the Stochastic Gradient Descent method with the ideal convergence rate $O(\frac{1}{T})$. Besides, our formulation is suitable for a wide spectrum of important loss functions in the literature of machine learning (i.e., Hinge, smooth Hinge, Logistic, L1, and ϵ -insensitive) and smoothness functions (i.e., $l_p(t) = |t|^p$ with $p \geq 1$). We further show that the well-known Laplacian Support Vector Machine is a special case of our formulation. We validate our proposed method on several benchmark datasets to demonstrate that GKM is appropriate for the large-scale datasets since it is optimal in memory usage and yields superior classification accuracy whilst simultaneously achieving a significant computation speed-up in comparison with the state-of-the-art baselines.

Keywords Semi-supervised Learning · Kernel Method · Support Vector Machine · Spectral Graph · Stochastic Gradient Descent

1 Introduction

Semi-supervised learning (SSL) aims at utilizing the intrinsic information carried in unlabeled data to enhance the generalization capacity of the learning algorithms. During the past decade, SSL has attracted significant attention and has found applicable in a variety of

Trung Le, Khanh Nguyen, Van Nguyen, Vu Nguyen, Dinh Phung
Centre for Pattern Recognition and Data Analytics, Deakin University, Australia
Tel.: +61-352479655
E-mail: {trung.l, khanh.n, van.n, v.nguyen, dinh.phung}@deakin.edu.au

real-world problems including text categorization Joachims [1999], image retrieval Wang et al. [2003], bioinformatics Kasabov et al. [2005], natural language processing Goutte et al. [2002] to name a few. While obtaining pre-defined labels is a labor-intensive and time-consuming process Chapelle et al. [2008], it is well known that unlabeled data, when being used in conjunction with a small amount of labeled data, can bring a remarkable improvement in classification accuracy Joachims [1999].

A notable approach to semi-supervised learning paradigm is to employ spectral graph in order to represent the adjacent and distributive information carried in data. Graph-based methods are nonparametric, discriminative, and transductive in nature. Typical graph-based methods include min-cut Blum et al. [2004], harmonic function Zhu et al. [2003], graph random walk Azran [2007], spectral graph transducer Joachims [2003], Duong et al. [2015], and manifold regularization Belkin et al. [2006].

Inspired from the pioneering work of Joachims [1999], recent works have attempted to incorporate kernel methods such as Support Vector Machine (SVM) Cortes and Vapnik [1995] with the semi-supervised learning paradigm. The underlying idea is to *solve the standard SVM problem while treating the unknown labels as optimization variables* Chapelle et al. [2008]. This leads to a non-convex optimization problem with a combinatorial explosion of label assignments. A wide spectrum of techniques have been proposed to solve this non-convex optimization problem, e.g., local combination search Joachims [1999], gradient descent Chapelle and Zien [2005], continuation techniques Chapelle et al. [2006], convex-concave procedures Collobert et al. [2006], deterministic annealing Sindhwani et al. [2006], Le et al. [2013], Nguyen et al. [2014], and semi-definite programming De Bie and Cristianini [2006]. Although these works can somehow handle the combinatorial intractability, their common requirement of repeatedly retraining the model limits their applicability to real-world applications, hence lacking the ability to perform online learning for large-scale applications.

Conjoining the advantages of kernel method and the spectral graph theory, several existing works have tried to incorporate information carried in a spectral graph for building a better kernel function Kondor and Lafferty [2002], Chapelle et al. [2003], Smola and Kondor [2003]. Basically, these methods employ the Laplacian matrix induced from the spectral graph to construct kernel functions which can capture the features of the ambient space. Manifold regularization framework Belkin et al. [2006] exploits the geometric information of the probability distribution that generates data and incorporates it as an additional regularization term. Two regularization terms are introduced to control the complexity of the classifier in the ambient space and the complexity induced from the geometric information of the distribution. However, the computational complexity for manifold regularization approach is cubic in the training size n (i.e., $O(n^3)$). Hence other researches have been carried out to enhance the scalability of the manifold regularization framework Sindhwani and Niyogi [2005], Tsang and Kwok [2006], Melacci and Belkin [2011]. Specifically, the work of Melacci and Belkin [2011] makes use of the preconditioned conjugate gradient to solve the optimization problem encountered in manifold regularization framework in the primal form, reducing the computational complexity from $O(n^3)$ to $O(n^2)$. However, this approach is not suitable for online learning setting since it actually solves the optimization problem in the first dual layer instead of the primal form. In addition, the LapSVM in primal approach Melacci and Belkin [2011] requires storing the entire Hessian matrix of size $n \times n$ in the memory, resulting in a memory complexity of $O(n^2)$. Our evaluating experiments with LapSVM in primal further show that it always consumes a huge amount of memory in its execution (cf. Table 5).

Recently, stochastic gradient descent (SGD) methods Shalev-shwartz and Singer [2007], Kakade and Shalev-Shwartz [2008], Lacoste-Julien et al. [2012] have emerged as a promising framework to speed up the training process and enable the online learning paradigm. SGD possesses three key advantages: (1) it is fast; (2) it can be exploited to run in online mode; and (3) it is efficient in memory usage. In this paper, we leverage the strength from three bodies of theories, namely kernel method, spectral graph theory and stochastic gradient descent to propose a novel approach to semi-supervised learning, termed as *Graph-based Semi-supervised Kernel Machine* (GKM). Our GKM is applicable for a wide spectrum of loss functions (cf. Section 5) and smoothness functions $l_p(\cdot)$ where $p \geq 1$ (cf. Eq. (4)). In addition, we note that the well-known Laplacian Support Vector Machine (LapSVM) Belkin et al. [2006], Melacci and Belkin [2011] is a special case of GKM(s) when using Hinge loss and the smoothness function $l_2(\cdot)$. We then develop a new algorithm based on the SGD framework Lacoste-Julien et al. [2012] to directly solve the optimization problem of GKM in its primal form with the ideal convergence rate $O(\frac{1}{T})$. At each iteration, a labeled instance and an edge in the spectral graph are randomly sampled. As the result, the computational cost at each iteration is very economic, hence making the proposed method efficient to deal with large-scale datasets while maintaining comparable predictive performance.

To summarize, our contributions in this paper are as follows:

- We provide a novel view of jointly learning the kernel method with a spectral graph for semi-supervised learning. Our proposed GKM enables the combination of a wide spectrum of convex loss functions and smoothness functions.
- We use the stochastic gradient descent (SGD) to solve directly GKM in its primal form. Hence, GKM has all advantageous properties of SGD-based methods including fast computation, memory efficiency, and online setting. To the best of our knowledge, the proposed GKM is *the first kernelized semi-supervised learning method* that can deal with the *online learning context* for large-scale application.
- We provide a theoretical analysis to show that GKM has the ideal convergence rate $O(\frac{1}{T})$ if the function is smooth and the loss function satisfies a proper condition. We then verify that this necessary condition holds for a wide class of loss functions including Hinge, smooth Hinge, and Logistic for classification task and L1, ϵ -insensitive for regression task (cf. Section 5).
- The experimental results further confirm the ideal convergence rate $O(\frac{1}{T})$ of GKM empirically and show that GKM is readily scalable for large-scale datasets. In particular, it offers a comparable classification accuracy whilst achieving a significant computational speed-up in comparison with the state-of-the-art baselines.

2 Related Work

We review the works in semi-supervised learning paradigm that are closely related to ours. Graph-based semi-supervised learning is an active research topic under semi-supervised learning paradigm. At its crux, graph-based semi-supervised methods define a graph where the vertices are labeled and unlabeled data of the training set and edges (may be weighted) reflect the similarity of data. Most of graph-based methods can be interpreted as estimating the prediction function f such that: it should predict the labeled data as accurate as possible; and it should be smooth on the graph.

In [Blum and Chawla, 2001, Blum et al., 2004], semi-supervised learning problem is viewed as graph mincut problem. In the binary case, positive labels act as *sources* and negative labels act as *sinks*. The objective is to find a minimum set of edges whose removal

blocks all flow from the sources to the sinks. Another way to infer the labels of unlabeled data is to compute the marginal probability of the discrete Markov random field. In [Zhu and Ghahramani, 2002], Markov Chain Monte Carlo sampling technique is used to approximate this marginal probability. The work of [Getz et al., 2006] proposes to compute the marginal probabilities of the discrete Markov random field at any temperature with the Multi-canonical Monte Carlo method, which seems to be able to overcome the energy trap faced by the standard Metropolis or Swendsen - Wang method. The harmonic functions used in [Zhu et al., 2003] is regarded as a continuous relaxation of the discrete Markov random field. It does relaxation on the value of the prediction function and makes use of the quadratic loss with infinite weight so that the labeled data are clamped. The works of [Kondor and Lafferty, 2002, Chapelle et al., 2003, Smola and Kondor, 2003] utilize the Laplacian matrix induced from the spectral graph to form kernel functions which can capture the features of the ambient space.

Yet another successful approach in semi-supervised learning paradigm is the kernel-based approach. The kernel-based semi-supervised methods are primarily driven by the idea to solve a standard SVM problem while treating the unknown labels as optimization variables [Chapelle et al., 2008]. This leads to a non-convex optimization problem with a combinatorial explosion of label assignments. Many methods have been proposed to solve this optimization problem, for example local combinatorial search [Joachims, 1999], gradient descent [Chapelle and Zien, 2005], continuation techniques [Chapelle et al., 2006], convex-concave procedures [Collobert et al., 2006], deterministic annealing [Sindhwani et al., 2006, Le et al., 2013, Nguyen et al., 2014], and semi-definite programming [De Bie and Cristianini, 2006]. However, the requirement of retraining the whole dataset over and over precludes the applications of these kernel-based semi-supervised methods to the large-scale and streaming real-world datasets.

Some recent works on semi-supervised learning have primarily concentrated on the improvements of its safeness and classification accuracy. Li and Zhou [2015] assumes that the low-density separators can be diverse and an incorrect selection may result in a reduced performance and then proposes S4VM to use multiple low-density separators to approximate the ground-truth decision boundary. S4VM is shown to be safe and to achieve the maximal performance improvement under the low-density assumption of S3VM [Joachims, 1999]. Wang et al. [2015] extends [Belkin et al., 2006, Wu et al., 2010] to propose semi-supervised discrimination-aware manifold regularization framework which considers the discrimination of all available instances in learning of manifold regularization. Tan et al. [2014] proposes using the p -norm as a regularization quantity in manifold regularization framework to perform the dimensionality reduction task in the context of semi-supervised learning.

The closest work to ours is the manifold regularization framework [Belkin et al., 2006] and its extensions [Sindhwani and Niyogi, 2005, Tsang and Kwok, 2006, Melacci and Belkin, 2011]. However, the original work of manifold regularization [Belkin et al., 2006] requires to invert a matrix of size n by n which costs cubically and hence is not scalable. Addressing this issue, Tsang and Kwok [2006] scales up the manifold regularization framework by adding in an ε -insensitive loss into the energy function, i.e., replacing $\sum w_{ij}(f(x_i) - f(x_j))^2$ by $\sum w_{ij}(|f(x_i) - f(x_j)|_\varepsilon)^2$, where $|z|_\varepsilon = \max\{|z| - \varepsilon, 0\}$. The intuition is that most pairwise differences $|f(x_i) - f(x_j)|$ are very small. By ignoring the differences smaller than ε , the solution becomes sparser. LapSVM (in primal) [Melacci and Belkin, 2011] employs the preconditioned conjugate gradient to solve the optimization problem of manifold regularization in the primal form. This allows the computational complexity to be scaled up from $O(n^3)$ to $O(n^2)$. However, the optimization problem in [Melacci and

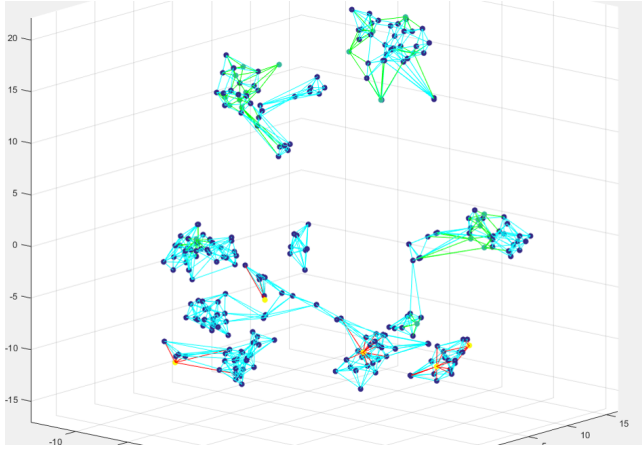


Fig. 1 Visualization of a spectral graph on 3D dataset using k -NN with $k = 5$.

Belkin, 2011] is indeed solved in the first dual layer rather than in the primal form. Furthermore, we empirically show that LapSVM in primal is expensive in terms of memory complexity (cf. Table 5).

Finally, the preliminary results of this work has been published in [Le et al., 2016] where it presents a special case of this work in which the combination of Hinge loss and the smoothness function $l_1(\cdot)$ is employed. In addition, our preliminary work [Le et al., 2016] guarantees only the convergence rate $O\left(\frac{\log T}{T}\right)$. In this work, we have substantially expanded [Le et al., 2016] and developed more powerful theory that guarantees the ideal convergence rate. We then further developed theory and analysis in order to enable the employment of a wide spectrum of loss and smoothness functions. Finally, we expanded significantly on the new technical contents, explanations as well as more extensive empirical studies.

3 Graph Setting for Semi-supervised Learning

Our *spectral graph* is defined as a pair $\mathcal{G} = (\mathcal{V}, \mathcal{E})$ comprising a set \mathcal{V} of vertices or nodes or points together with a set \mathcal{E} of edges or arcs or lines, which are 2-element subsets of V (i.e. an edge is associated with two vertices, and that association takes the form of the unordered pair comprising those two vertices). In the context of semi-supervised learning, we are given a training set $X = X_l \cup X_u$ where $X_l = \{(x_i, y_i)\}_{i=1}^l$ is labeled data and $X_u = \{x_i\}_{i=l+1}^{l+u}$ is unlabeled data. We construct the vertex set \mathcal{V} includes all labeled and unlabeled instances (i.e., $\mathcal{V} = \{x_i\}_{i=1}^{l+u}$). An edge $e_{ij} = \overline{x_i x_j} \in \mathcal{E}$ between two vertices x_i, x_j represents the similarity of the two instances. Let μ_{ij} be the weight associated with edge e_{ij} . The underlying principle is to enforce that if μ_{ij} is large, then y_i and y_j are expected to receive the same label. The set of edges \mathcal{E} and its weights can be built using the following ways [Zhu et al., 2009, Le et al., 2016]:

- *Fully connected graph*: every pair of vertices x_i, x_j is connected by an edge. The edge weight decreases when the distance $\|x_i - x_j\|$ increases. The Gaussian kernel function widely used is given by $\mu_{ij} = \exp\left(-\|x_i - x_j\|^2 / (2\sigma_s^2)\right)$ where σ_s controls how quickly the weight decreases.

- k -NN: each vertex x_i determines its k nearest neighbors (k -NN) and makes an edge with each of its k -NN. The Gaussian kernel weight function can be used for the edge weight. Empirically, k -NN graphs with small k tend to perform well.
- ε -NN: we connect x_i and x_j if $\|x_i - x_j\| \leq \varepsilon$. Again the Gaussian kernel weight function can be used to weight the connected edges. In practice, ε -NN graphs are easier to construct than k -NN graphs.

When constructing a graph, we avoid connecting the edge of two labeled instances since we do not need to propagate the label between them. Figure 1 illustrates an example of graph constructed on 3D dataset using k -NN with $k = 5$.

After constructing a graph, we formulate a semi-supervised learning problem as assigning labels to the unlabeled vertices via *label propagation*. We propagate the labels from the labeled vertices to the unlabeled ones by encouraging y_i to have the same label as y_j if the weight μ_{ij} is large and vice versa. To do so, we learn a mapping function $f: \mathcal{X} \rightarrow \mathcal{Y}$ where \mathcal{X} and \mathcal{Y} are the domains of data and label such that

- $f(x_i)$ is as close to its label y_i as possible for all labeled instances x_i ($1 \leq i \leq l$).
- f should be smooth on the graph \mathcal{G} , i.e., if x_i is very close to x_j (i.e., μ_{ij} is large), the discrepancy between f_i and f_j (i.e., $|f_i - f_j|$) is small.

Therefore, we obtain the optimization problem [Zhu et al., 2009, Le et al., 2016] as

$$\min_f \left(\infty \times \sum_{i=1}^l (f(x_i) - y_i)^2 + \sum_{(i,j) \in \mathcal{E}} \mu_{ij} (f(x_i) - f(x_j))^2 \right) \quad (1)$$

where by convention we define $\infty \times 0 = 0$. The optimization problem in Eq. (1) get the minimum when the first term is 0 and the second term is as smallest as possible. We rewrite the optimization problem in Eq. (1) into a constrained optimization problem to link it to SVM-based optimization problem for semi-supervised learning:

$$\min_f \left(\sum_{(i,j) \in \mathcal{E}} \mu_{ij} (f(x_i) - f(x_j))^2 \right) \quad \text{s.t.} : \forall_{i=1}^l : f(x_i) = y_i \quad (2)$$

To extend the representation ability of the prediction function f , we relax the discrete function f to be real-valued. The drawback of the relaxation is that in the solution, $f(x)$ is now real-valued and hence does not directly correspond to a label. This can however be addressed by thresholding $f(x)$ at zero to produce discrete label predictions, i.e., if $f(x) \geq 0$, predict $y = 1$, and if $f(x) < 0$, predict $y = -1$.

4 Graph-based Semi-supervised Kernel Machine

In this section, we present our proposed *Graph-based Semi-supervised Kernel Machine* (GKM). We begin with formulating the optimization problem for GKM, followed by the derivation of an SGD-based solution. Finally, we present the convergence analysis for our proposed method. The convergence analysis shows that our proposed method gains the ideal convergence rate $O(\frac{1}{T})$ for combinations of the typical loss functions (cf. Section 5) and the smoothness functions with $p \geq 1$.

4.1 GKM Optimization Problem

Let $\Phi : \mathcal{X} \rightarrow \mathcal{H}$ be a transformation from the input space \mathcal{X} to a RHKS \mathcal{H} . To predict label, we use the function $f(x) = \mathbf{w}^\top \Phi(x) - \rho = \sum_{i=1}^{l+u} \alpha_i K(x_i, x) - \rho$, where $\mathbf{w} = \sum_{i=1}^{l+u} \alpha_i \Phi(x_i)$. Continuing from the constrained optimization problem in Eq. (2), we propose the following optimization problem over a graph [Le et al., 2016]

$$\begin{aligned} \min_{\mathbf{w}} & \left(\frac{1}{2} \|\mathbf{w}\|^2 + \frac{C}{l} \sum_{i=1}^l \xi_i + \frac{C'}{|\mathcal{E}|} \sum_{(i,j) \in \mathcal{E}} \mu_{ij} (f(x_i) - f(x_j))^2 \right) \\ \text{s.t.} & : \forall_{i=1}^l : y_i (\mathbf{w}^\top \Phi(x_i) - \rho) \geq 1 - \xi_i; \quad \text{and} \quad \forall_{i=1}^l : \xi_i \geq 0 \end{aligned} \quad (3)$$

where $f(x_i) = \mathbf{w}^\top \Phi(x_i) - \rho$. The optimization problem in Eq. (3) can be intuitively understood as follows. We minimize $\frac{1}{2} \|\mathbf{w}\|^2$ to maximize the margin to promote the generalization capacity, similar to the intuition of SVM [Cortes and Vapnik, 1995]. At the same time, we minimize $\sum_{(i,j) \in \mathcal{E}} \mu_{ij} (f(x_i) - f(x_j))^2$ to make the prediction function smoother on the spectral graph. We rewrite the optimization problem in Eq. (3) in the primal form as¹

$$\min_{\mathbf{w}} \left(\frac{\|\mathbf{w}\|^2}{2} + \frac{C}{l} \sum_{i=1}^l l(\mathbf{w}; z_i) + \frac{C'}{|\mathcal{E}|} \sum_{(i,j) \in \mathcal{E}} \mu_{ij} l_2(\mathbf{w}^\top \Phi_{ij}) \right) \quad (4)$$

where $z_i = (x_i, y_i)$, $l(\mathbf{w}; x, y) = \max\{0, 1 - y\mathbf{w}^\top \Phi(x)\}$, $\Phi_{ij} = \Phi(x_i) - \Phi(x_j)$, $l_p(t) = |t|^p$ with $t \in \mathbb{R}$, and $p \geq 1$. In the optimization problem in Eq. (4), the minimization of $\sum_{i=1}^l l(\mathbf{w}; x_i, y_i)$ encourages the fitness of GKM on the labeled portion while the minimization of $\sum_{(i,j) \in \mathcal{E}} \mu_{ij} l_2(\mathbf{w}^\top \Phi_{ij})$ guarantees the smoothness of GKM on the spectral graph. Naturally, we can extend the optimization of GKM by replacing the Hinge loss by any loss function and $l_2(\cdot)$ by $l_p(\cdot)$ with $p \geq 1$.

We note that Laplacian Support Vector Machine (LapSVM) [Belkin et al., 2006, Melacci and Belkin, 2011] is a special case of GKM using the Hinge loss with the smoothness function $l_2(\cdot)$.

4.2 Stochastic Gradient Descent Algorithm for GKM

We employ the SGD framework [Lacoste-Julien et al., 2012] to solve the optimization problem in Eq. (4) in the primal form. Let us denote the objective function as

$$\mathcal{J}(\mathbf{w}) \triangleq \frac{\|\mathbf{w}\|^2}{2} + \frac{C}{l} \sum_{i=1}^l l(\mathbf{w}; x_i, y_i) + \frac{C'}{|\mathcal{E}|} \sum_{(i,j) \in \mathcal{E}} \mu_{ij} l_p(\mathbf{w}^\top \Phi_{ij})$$

At the iteration t , we do the following:

- Uniformly sample a labeled instance x_{i_t} ($1 \leq i_t \leq l$) from the labeled portion X_l and an edge (u_t, v_t) from the set of edges \mathcal{E} .
- Define the instantaneous objective function

$$\mathcal{J}_t(\mathbf{w}) = \frac{\|\mathbf{w}\|^2}{2} + Cl(\mathbf{w}; x_{i_t}, y_{i_t}) + C' \mu_{u_t v_t} l_p(\mathbf{w}^\top \Phi_{u_t v_t})$$

¹ We can eliminate the bias ρ by simply adjusting the kernel.

- Define the stochastic gradient $g_t = \nabla_{\mathbf{w}} \mathcal{J}_t(\mathbf{w}_t)$

$$g_t = \mathbf{w}_t + C \nabla_{\mathbf{w}} l(\mathbf{w}_t; x_{i_t}, y_{i_t}) + C' \mu_{u_t v_t} \nabla_{\mathbf{w}} l_p(\mathbf{w}_t^{\top} \Phi_{u_t v_t})$$

where $\nabla_{\mathbf{w}} l(\mathbf{w}; x, y)$ specifies the derivative or sub-gradient w.r.t. \mathbf{w} .

- Update \mathbf{w}_{t+1} with the learning rate $\eta_t = \frac{2}{t+1}$, $\mathbf{w}_{t+1} = \mathbf{w}_t - \eta_t g_t$

$$\mathbf{w}_{t+1} = \frac{t-1}{t+1} \mathbf{w}_t - \frac{2C}{t+1} \nabla_{\mathbf{w}} l(\mathbf{w}_t; x_{i_t}, y_{i_t}) - \frac{2C' \mu_{u_t v_t}}{t+1} \nabla_{\mathbf{w}} l_p(\mathbf{w}_t^{\top} \Phi_{u_t v_t})$$

- Update $\bar{\mathbf{w}}_{t+1} = \frac{t-1}{t+1} \bar{\mathbf{w}}_t + \frac{2}{t+1} \mathbf{w}_{t+1}$

We note that the derivative $\nabla_{\mathbf{w}} l_p(\mathbf{w}^{\top} \Phi)$ w.r.t. \mathbf{w} can be computed as

$$\nabla_{\mathbf{w}} l_p(\mathbf{w}^{\top} \Phi) = p \text{sign}(\mathbf{w}^{\top} \Phi) |\mathbf{w}^{\top} \Phi|^{p-1} \Phi$$

Algorithm 1 Algorithm for GKM.

Input : $C, C', p, K(\cdot, \cdot)$

- 1: $\mathbf{w}_1 = \mathbf{0}, \bar{\mathbf{w}}_1 = \mathbf{0}$
- 2: **for** $t = 1$ **to** T **do**
- 3: Uniformly sample i_t from $\{1, 2, \dots, l\}$ and (u_t, v_t) from the set of edges \mathcal{E}
- 4: Update $\mathbf{w}_{t+1} = \frac{t-1}{t+1} \mathbf{w}_t - \frac{2C}{t+1} \nabla_{\mathbf{w}} l(\mathbf{w}_t; x_{i_t}, y_{i_t}) - \frac{2C' \mu_{u_t v_t}}{t+1} \nabla_{\mathbf{w}} l_p(\mathbf{w}_t^{\top} \Phi_{u_t v_t})$
- 5: Update $\bar{\mathbf{w}}_{t+1} = \frac{t-1}{t+1} \bar{\mathbf{w}}_t + \frac{2}{t+1} \mathbf{w}_{t+1}$
- 6: **end for**

Output : $\bar{\mathbf{w}}_{T+1}$

The pseudocode of GKM is presented in Algorithm 1. We note that we store \mathbf{w}_t and $\bar{\mathbf{w}}_t$ as $\mathbf{w}_t = \sum_i \alpha_i \Phi(x_i)$ and $\bar{\mathbf{w}}_t = \sum_i \beta_i \Phi(x_i)$. In line 5 of Algorithm 1, the update of \mathbf{w}_{t+1} involves the coefficients of $\Phi(x_{i_t})$, $\Phi(x_{u_t})$, and $\Phi(x_{v_t})$. In line 4 of Algorithm 1, we need to sample the edge (u_t, v_t) from the set of edges \mathcal{E} and compute the edge weight $\mu_{u_t v_t}$. It is noteworthy that in GKM we use the fully connected spectral graph to maximize the freedom of label propagation and avoid the additional computation incurred in other kind of spectral graph (e.g., k -NN or ε -NN spectral graph). In addition, the edge weight $\mu_{u_t v_t}$ can be computed on the fly when necessary.

4.3 Convergence Analysis

After presenting the SGD algorithm for our proposed GKM, we now present the convergence analysis. In particular, assuming that the loss function satisfies the condition: $\|\nabla_{\mathbf{w}} l(\mathbf{w}; x, y)\| \leq A, \forall x, y$, we prove that our GKM achieves the ideal convergence rate $O(\frac{1}{T})$ with $1 \leq p < 2$ and with $p \geq 2$ under some condition of the parameters (cf. Theorem 1) while we note that the previous work of [Le et al., 2016] achieves a convergence rate of $O(\frac{\log T}{T})$. We present the theoretical results and the rigorous proofs are given in Appendix A. Without loss of generality, we assume that the feature map $\Phi(x)$ is bounded in the feature space, i.e., $\|\Phi(x)\| = K(x, x)^{1/2} \leq R, \forall x$. We denote the optimal solution by \mathbf{w}^* , i.e., $\mathbf{w}^* = \text{argmin}_{\mathbf{w}} J(\mathbf{w})$.

The following lemma shows the formula for $\bar{\mathbf{w}}_t$ from its recursive formula.

Lemma 1 We have the following statement $\bar{\mathbf{w}}_t = \frac{2}{t(t-1)} \sum_{i=1}^{t-1} i \mathbf{w}_i$.

Lemma 2 further offers the foundation to establish an upper bound for $\|\mathbf{w}_t\|$.

Lemma 2 Let us consider the function $f(x; a, b, p) = ax^{p-1} - x + b$ where $x \geq 0$ and $p \geq 1$, $a, b > 0$. The following statements are guaranteed

- i) If $p < 2$ then $f(M; a, b, p) \leq 0$ where $M = \max\left(1, (a+b)^{\frac{1}{2-p}}\right)$.
- ii) If $p = 2$ and $a < 1$ then $f(M; a, b, p) \leq 0$ where $M = \frac{b}{1-a}$.
- iii) If $p > 2$ and $ab^{p-2} \leq \frac{(p-2)^{p-2}}{(p-1)^{p-1}}$ then $f(M; a, b, p) \leq 0$ where $M = \left(\frac{1}{(p-1)a}\right)^{\frac{1}{p-2}}$.

Built on the previous lemma, Lemma 3 establishes an upper bound on $\|\mathbf{w}_t\|$ which is used to define the bound in Lemma 4.

Lemma 3 We have the following statement $\|\mathbf{w}_t\| \leq M, \forall t$ where M is defined as

$$M = \begin{cases} \max\left(1, (a+b)^{\frac{1}{2-p}}\right) & \text{if } p < 2 \\ \frac{b}{1-a} & \text{if } p = 2, a < 1 \\ \left(\frac{1}{(p-1)a}\right)^{\frac{1}{p-2}} & \text{if } p > 2, ab^{p-2} \leq \frac{(p-2)^{p-2}}{(p-1)^{p-1}} \end{cases}$$

with $a = C'(2R)^p p$ and $b = CA$.

Lemma 4 establishes an upper bound on $\|g_t\|$ for our subsequent theorems.

Lemma 4 We have $\|g_t\| \leq G, \forall t$ where $G = M + CA + C'(2R)^p p M^{p-1}$.

We now turn to establish the ideal convergence rate $O\left(\frac{1}{T}\right)$ for our proposed GKM.

Theorem 1 Considering the running of Algorithm 1, the following statements hold

- i) $\mathbb{E}[\mathcal{J}(\bar{\mathbf{w}}_{T+1})] - \mathcal{J}(\mathbf{w}^*) \leq \frac{2G^2}{T}, \forall T$
- ii) $\mathbb{E}\left[\|\bar{\mathbf{w}}_{T+1} - \mathbf{w}^*\|^2\right] \leq \frac{4G^2}{T}, \forall T$

if $1 \leq p < 2$ or $p = 2, a < 1$ or $p > 2, ab^{p-2} \leq \frac{(p-2)^{p-2}}{(p-1)^{p-1}}$ where $a = C'(2R)^p p$ and $b = CA$.

Theorem 1 states the regret in the form of expectation. We go further to prove that for all $T \geq T_0 = \left\lceil \frac{2G^2}{\varepsilon\delta} \right\rceil$, with a high confidence level, $\mathcal{J}(\bar{\mathbf{w}}_{T+1})$ approximates the optimal value $\mathcal{J}(\mathbf{w}^*)$ within an ε -precision in Theorem 2.

Theorem 2 With the probability $1 - \delta, \forall T \geq T_0 = \left\lceil \frac{2G^2}{\varepsilon\delta} \right\rceil$, $\mathcal{J}(\bar{\mathbf{w}}_{T+1})$ approximates the optimal value $\mathcal{J}(\mathbf{w}^*)$ within ε -precision, i.e., $\mathcal{J}(\bar{\mathbf{w}}_{T+1}) \leq \mathcal{J}(\mathbf{w}^*) + \varepsilon$ if $1 \leq p < 2$ or $p = 2, a < 1$ or $p > 2, ab^{p-2} \leq \frac{(p-2)^{p-2}}{(p-1)^{p-1}}$ where $a = C'(2R)^p p$ and $b = CA$.

5 Suitability of Loss Function and Kernel Function

In this section, we present the suitability of five loss and kernel functions that can be used for GKM including hinge, smooth hinge, logistic, L1, and ε -insensitive. We verify that most of the well-known loss functions satisfy the necessary condition: $\|\nabla_{\mathbf{w}}l(\mathbf{w};x,y)\| \leq A$ for an appropriate positive number A . By allowing multiple choices of loss functions, we enable broader applicability of the proposed GKM for real-world applications while the work of [Le et al., 2016] is restricted to a Hinge loss function.

– *Hinge loss*: $l(\mathbf{w};x,y) = \max\{0, 1 - y\mathbf{w}^\top \Phi(x)\}$,

$$\nabla_{\mathbf{w}}l(\mathbf{w};x,y) = -\mathbb{I}_{\{y\mathbf{w}^\top \Phi(x) \leq 1\}} y \Phi(x)$$

Therefore, by choosing $A = R$ we have $\|\nabla_{\mathbf{w}}l(\mathbf{w};x,y)\| \leq \|\Phi(x)\| \leq R = A$.

– *Smooth Hinge loss* [Shalev-Shwartz and Zhang, 2013]:

$$l(\mathbf{w};x,y) = \begin{cases} 0 & \text{if } yo > 1 \\ 1 - y\mathbf{w}^\top \Phi(x) - \frac{\tau}{2} & \text{if } yo < 1 - \tau \\ \frac{1}{2\tau}(1 - yo)^2 & \text{otherwise} \end{cases}$$

$$\nabla_{\mathbf{w}}l(\mathbf{w};x,y) = -\mathbb{I}_{\{yo < 1 - \tau\}} y \Phi(x) + \tau^{-1} \mathbb{I}_{1 - \tau \leq yo \leq 1} (yo - 1) y \Phi(x)$$

where $o = \mathbf{w}^\top \Phi(x)$. Therefore, by choosing $A = R$ we have

$$\begin{aligned} \|\nabla_{\mathbf{w}}l(\mathbf{w};x,y)\| &= R \left| \tau^{-1} \mathbb{I}_{1 - \tau \leq yo \leq 1} (yo - 1) \right| + R \mathbb{I}_{\{yo < 1 - \tau\}} \\ &\leq \mathbb{I}_{\{yo < 1 - \tau\}} R + \tau^{-1} \mathbb{I}_{1 - \tau \leq yo \leq 1} R \leq R = A \end{aligned}$$

– *Logistic loss*: $l(\mathbf{w};x,y) = \log(1 + \exp(-y\mathbf{w}^\top \Phi(x)))$,

$$\nabla_{\mathbf{w}}l(\mathbf{w};x,y) = \frac{-y \exp(-y\mathbf{w}^\top \Phi(x)) \Phi(x)}{\exp(-y\mathbf{w}^\top \Phi(x)) + 1}$$

By choosing $A = R$ we have $\|\nabla_{\mathbf{w}}l(\mathbf{w};x,y)\| < \|\Phi(x)\| \leq R = A$.

– *L1 loss*: $l(\mathbf{w};x,y) = |y - \mathbf{w}^\top \Phi(x)|$, $\nabla_{\mathbf{w}}l(\mathbf{w};x,y) = \text{sign}(\mathbf{w}^\top \Phi(x) - y) \Phi(x)$. By choosing $A = R$ we have $\|\nabla_{\mathbf{w}}l(\mathbf{w};x,y)\| \leq \|\Phi(x)\| \leq R = A$.

– *ε -insensitive loss*: let denote $o = \mathbf{w}^\top \Phi(x)$, $l(\mathbf{w};x,y) = \max\{0, |y - \mathbf{w}^\top \Phi(x)| - \varepsilon\}$,

$$\nabla_{\mathbf{w}}l(\mathbf{w};x,y) = \mathbb{I}_{\{|y - o| > \varepsilon\}} \text{sign}(o - y) \Phi(x)$$

By choosing $A = R$ we have $\|\nabla_{\mathbf{w}}l(\mathbf{w};x,y)\| \leq \|\Phi(x)\| \leq R = A$.

Here, \mathbb{I}_S is the indicator function which is equal to 1 if the statement S is true and 0 if otherwise. It can be observed that the positive constant A coincides the radius R (i.e., $A = R$) for the aforementioned loss functions. To allow the ability to flexibly control the minimal sphere that encloses all $\Phi(x)$ (s), we propose to use the squared exponential (SE) kernel function $k(x, x') = \sigma_f^2 \exp(-\|x - x'\|^2 / (2\sigma_l^2))$ where σ_l is the length-scale and σ_f is the output variance parameter. Using SE kernel, we have the following equality $\|\Phi(x)\| = K(x, x)^{1/2} = \sigma_f \leq R$. Recall that if $p = 2$ or $p > 2$, Algorithm 1 converges to the optimal solution with the ideal convergence rate $O(\frac{1}{T})$ under specific conditions. In particular, with $p = 2$ the corresponding condition is $a < 1$ and with $p > 2$ the corresponding condition is $ab^{p-2} \leq \frac{(p-2)^{p-2}}{(p-1)^{p-1}}$ where $a = C'(2R)^p p$ and $b = CA$. Using the SE kernel, we can adjust the output variance parameter σ_f to make the convergent condition valid. More specifically, we consider two cases:

- $p = 2$: we have $a < 1 \rightarrow C' (2R)^p p < 1 \rightarrow R < 0.5 (pC')^{-1/p}$. We can simply choose σ_f with a very small number $\rho > 0$

$$\sigma_f = R = 0.5 (pC')^{-1/p} - \rho = 0.5 (2C')^{-1/2} - \rho$$

- $p > 2$: we have $ab^{p-2} \leq (p-2)^{p-2} (p-1)^{1-p}$ and then

$$C' (2R)^p p (CA)^{p-2} \leq (p-2)^{p-2} (p-1)^{1-p}$$

$$R \leq \left(\frac{(p-2)^{p-2}}{2^p C^{p-2} C' p (p-1)^{p-1}} \right)^{\frac{1}{2p-2}}$$

We can simply choose $\sigma_f = R = \left(\frac{(p-2)^{p-2}}{2^p C^{p-2} C' p (p-1)^{p-1}} \right)^{\frac{1}{2p-2}}$.

We can control the second trade-off parameter C' to ensure the ideal convergence rate $O\left(\frac{1}{T}\right)$ with $p \geq 2$. More specifically, we also consider two cases:

- $p = 2$: we have $a < 1 \rightarrow C' < (2R)^{-p} p^{-1} = 0.125$.
- $p > 2$: we have $ab^{p-2} \leq (p-2)^{p-2} (p-1)^{1-p}$ and thus

$$C' \leq \frac{(p-2)^{p-2}}{2^p C^{p-2} p (p-1)^{p-1}} \quad (5)$$

6 Experiments

We conduct the extensive experiments to investigate the influence of the model parameters and other factors to the model behavior and to compare our proposed GKM with the state-of-the-art baselines on the benchmark datasets. In particular, we design three kinds of experiments to analyze the influence of factors (e.g., the loss function, the smoothness function, and the percentage of unlabeled portion) to the model behavior. In the first experiment (cf. Section 6.1.1), we empirically demonstrate the theoretical convergence rate $O\left(\frac{1}{T}\right)$ for all combinations of loss function (Hinge and Logistic) and smoothness function ($p = 1, 2, 3$) and also investigate how the number of

iterations affects the classification accuracy. In the second experiment (cf. Section 6.1.2), we study the influence of the loss function and the smoothness function to the predictive performance and the training time when the percentage of unlabeled portion is either 80% or 90%. In the third experiment (cf. Section 6.1.3), we examine the proposed method under the semi-supervised setting where the proportion of unlabeled data is varied from 50% to 90%. Finally, we compare our proposed GKM with the state-of-the-art baselines on the benchmark datasets.

Dataset	Size	Dimension
COIL20	145	1,014
G50C	551	50
USPST	601	256
AUSTRALIAN	690	14
A1A	1,605	123
SVMGUIDE3	1,243	21
SVMGUIDE1	3,089	4
MUSHROOMS	8,124	112
W5A	9,888	300
W8A	49,749	300
IJCNN1	49,990	22
COD-RNA	59,535	8
COVTYPE	581,012	54

Table 1 Statistics for datasets used.

Datasets We use 13 benchmark datasets² (see Table 1 for details) for experiments on semi-supervised learning.

Baselines To investigate the efficiency and accuracy of our proposed method, we make comparison with the following baselines which, to the best of our knowledge, represent the state-of-the-art semi-supervised learning methods:

- *LapSVM in primal* [Melacci and Belkin, 2011]: Laplacian Support Vector Machine in primal is a state-of-the-art approach in semi-supervised classification based on manifold regularization framework. It can reduce the computational complexity of the original LapSVM [Belkin et al., 2006] from $O(n^3)$ to $O(kn^2)$ using the preconditioned conjugate gradient and an early stopping strategy.
- *CCCP* [Collobert et al., 2006]: It solves the non-convex optimization problem encountered in the kernel semi-supervised approach using convex-concave procedures.
- *Self-KNN* [Zhu et al., 2009]: Self-training is one of the most classical technique used in semi-supervised classification. Self-KNN employs k -NN method as a core classifier for self-training.
- *SVM*: Support Vector Machine which is implemented using LIBSVM solver [Chang and Lin, 2011] and trained with fully label setting. We use fully labeled SVM as a milestone to judge how good the semi-supervised methods are.

All compared methods are run on a Windows computer with the configuration of CPU Xeon 3.47 GHz and 96GB RAM. All codes of baseline methods are obtained from the corresponding authors.

6.1 Model Analysis

6.1.1 Convergence Rate Analysis

We empirically examine the convergence rate of GKM with various combinations of loss functions (Hinge, Logistic) and smooth functions ($p = 1, 2, 3$). We select G50C dataset which we compute the quantity $\Delta \mathcal{J} \mathcal{T} = (\mathcal{J}(\bar{\mathbf{w}}_{T+1}) - \mathcal{J}(\mathbf{w}^*)) \times T$ and measure the accuracy when the number of iterations T is varied. We repeat each experiment five times to record the necessary quantities and their standard deviations.

As observed from Figures 2, $\Delta \mathcal{J} \mathcal{T}$ tends to decrease and when T is sufficiently large, this quantity is upper-bounded by a constant. Hence, we can empirically conclude the convergence rate $O(\frac{1}{T})$ of GKM. Empirical result is consistent with the theoretical analysis developed in Section 4.3. We use the RBF kernel and with $p = 2$ and $p = 3$ the second trade-off parameter C' is selected using Eqs. (5) to theoretically guarantee the ideal convergence rate $O(\frac{1}{T})$ of our GKM.

6.1.2 Loss Functions and Smoothness Functions Analysis

This experiment aims to investigate how the variation in loss function and smoothness function affects the learning performance on real datasets. We experiment on the real datasets given in Table 1 with different combinations of loss function (e.g., Hinge, Logistic) and

² Most of the experimental datasets can be conveniently downloaded from the URL <https://www.csie.ntu.edu.tw/~cjlin/libsvmtools/datasets/>.

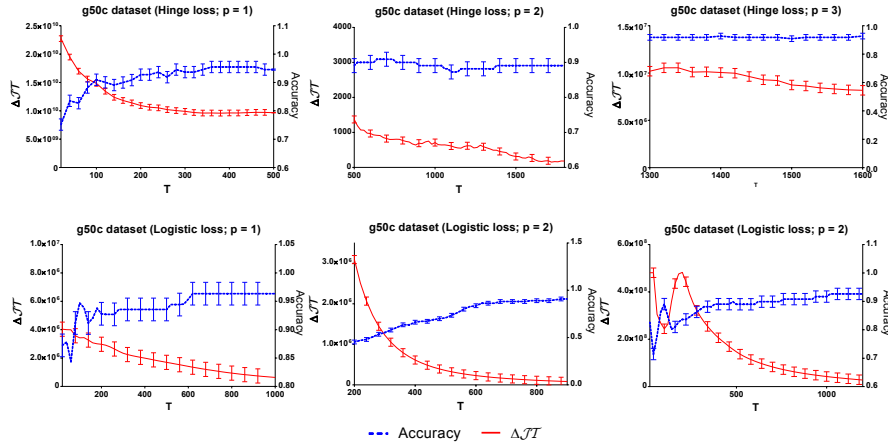


Fig. 2 Convergence analysis on the dataset G50C using the accuracy and the quantity $\Delta \mathcal{J} \mathcal{T} = (\mathcal{J}(\bar{\mathbf{w}}_{T+1}) - \mathcal{J}(\mathbf{w}^*)) \times T$. Hinge and Logistic losses are combined with $p = 1, 2, 3$. When T increases, the accuracy gradually improves and the quantity $\Delta \mathcal{J} \mathcal{T}$ decreases to a constant.

Dataset	Accuracy (%)						Time (s)					
	Hinge loss			Logistic loss			Hinge loss			Logistic loss		
	$p=1$	$p=2$	$p=3$	$p=1$	$p=2$	$p=3$	$p=1$	$p=2$	$p=3$	$p=1$	$p=2$	$p=3$
A1A	80.69	81.00	79.54	80.37	80.17	80.37	0.078	0.073	0.073	0.073	0.073	0.078
AUSTRALIAN	91.30	91.30	90.58	91.30	90.10	90.58	0.026	0.021	0.026	0.021	0.016	0.016
COIL20	100	100	100	100	100	100	0.010	0.010	0.015	0.005	0.015	0.010
G50C	92.73	95.45	95.45	95.45	95.45	95.45	0.026	0.015	0.031	0.021	0.015	0.021
SVM2	89.55	88.06	89.55	89.55	80.60	76.12	0.010	0.010	0.011	0.015	0.010	0.005
SVM3	81.85	80.24	80.24	79.84	81.05	79.30	0.125	0.015	0.015	0.015	0.015	0.015
USPST	99.17	99.17	99.17	99.17	99.17	99.17	0.032	0.031	0.037	0.037	0.031	0.036
COD-RNA	87.25	87.43	86.32	87.05	87.04	87.26	1.432	0.995	0.891	1.011	1.094	1.573
COVTYPE	84.15	83.89	79.81	78.78	78.93	78.61	1.599	1.422	1.755	1.760	1.510	1.594
IJCNN1	93.16	93.12	93.07	93.11	92.70	93.14	1.594	0.672	0.665	1.937	1.359	0.703
W5A	97.57	97.59	97.52	97.61	97.69	97.39	0.041	0.031	0.047	0.036	0.041	0.031
W8A	97.90	97.42	97.34	97.41	97.40	97.22	1.140	0.073	0.073	0.067	0.062	0.052
MUSHROOM	99.96	99.94	99.98	100	99.98	99.98	0.042	0.031	0.036	0.042	0.031	0.031

Table 2 The classification performance comparison when the hidden labeled data is 80%.

Dataset	Accuracy (%)						Time (s)					
	Hinge loss			Logistic loss			Hinge loss			Logistic loss		
	$p=1$	$p=2$	$p=3$	$p=1$	$p=2$	$p=3$	$p=1$	$p=2$	$p=3$	$p=1$	$p=2$	$p=3$
A1A	83.18	83.49	83.49	83.18	83.18	82.24	0.078	0.078	0.073	0.078	0.078	0.067
AUSTRALIAN	90.58	90.10	89.86	89.86	90.58	89.86	0.016	0.026	0.016	0.016	0.021	0.016
COIL	100	100	100	100	100	100	0.015	0.005	0.015	0.015	0.015	0.010
G50C	97.27	96.36	96.36	96.36	96.36	96.36	0.020	0.015	0.031	0.021	0.015	0.021
SVM2	82.09	82.09	80.60	73.63	79.10	73.13	0.010	0.010	0.015	0.005	0.010	0.010
SVM3	82.26	81.05	80.65	80.24	79.97	79.43	0.094	0.015	0.015	0.057	0.015	0.151
USPST	100	100	100	100	100	100	0.037	0.031	0.031	0.031	0.031	0.031
COD-RNA	87.37	87.51	87.07	87.38	87.23	86.18	0.974	1.115	0.896	1.078	1.000	0.865
COVTYPE	85.22	85.29	73.07	64.40	70.09	68.20	1.588	1.510	1.536	1.922	1.724	1.515
IJCNN1	92.84	92.62	92.82	92.59	92.63	92.50	0.641	0.729	0.774	1.135	1.158	0.734
W5A	97.64	97.61	97.50	97.69	97.47	97.49	0.036	0.052	0.052	0.052	0.052	0.041
W8A	98.00	97.50	97.60	97.56	97.48	97.35	0.677	0.068	0.146	0.146	0.385	0.088
MUSHROOM	99.92	99.96	99.96	100	99.96	99.94	0.172	0.037	0.031	0.032	0.031	0.032

Table 3 The classification performance comparison when the hidden labeled data is 90%.

Dataset	Accuracy (%)					F1 score (%)				
	50%	60%	70%	80%	90%	50%	60%	70%	80%	90%
G50C	98.21	95.45	95.02	94.29	93.82	98.19	95.51	94.97	93.02	93.02
COIL20	100	100	100	100	100	100	100	100	100	100
USPST	99.5	100	99.67	99.50	99.40	99.44	100	99.61	99.44	99.44
AUSTRALIAN	87.18	86.67	87.07	86.38	86.06	85.47	84.80	85.51	84.09	84.09
A1A	83.75	83.08	82.89	83.13	83.10	61.25	59.06	58.99	59.10	59.10
MUSHROOMS	100	100	99.99	100	100	99.9	100	99.99	100	100
SVMGUIDE3	87.35	77.55	77.83	78.20	77.36	78.01	20.06	22.25	22.81	22.81
W5A	91.128	88.40	88.11	87.29	87.92	86.02	81.50	81.24	79.30	79.30
W8A	97.29	97.29	97.27	97.25	97.29	11.46	11.62	10.81	10.33	10.33
COD-RNA	97.39	97.42	97.36	97.40	97.36	22.61	21.15	20.23	22.41	22.41
IJCNN1	89.59	87.44	87.20	87.22	88.52	80.87	79.74	79.53	79.56	79.56
COVTYPE	87.71	80.99	81.03	80.90	80.79	89.05	85.63	85.64	85.54	85.54

Table 4 The classification performance w.r.t. different fraction of unlabeled data.

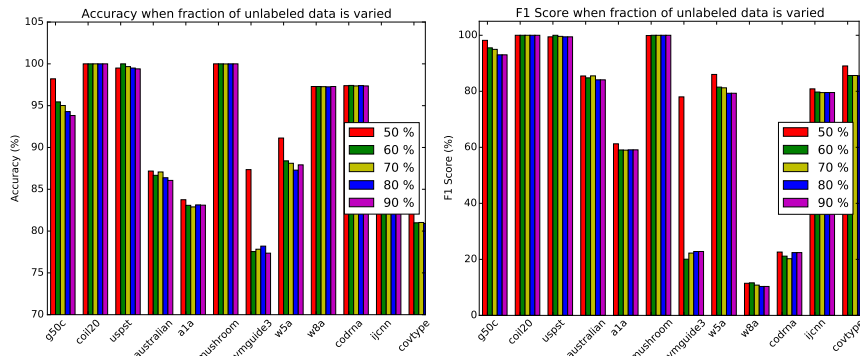


Fig. 3 Left: The classification accuracy when fraction of unlabeled data is varied. Right: The F1 score when fraction of unlabeled data is varied.

smoothness function (e.g., $p = 1, 2, 3$). Each experiment is performed five times and the average accuracy and training time corresponding to 80% and 90% of unlabeled data are reported in Tables 2 and 3 respectively. We observe that the Hinge loss is slightly better than Logistic one and the combination of Hinge loss and the smoothness $l_1(\cdot)$ is the best combination among others. It is noteworthy that in this simulation study we use the RBF kernel and with $p = 2$ and $p = 3$ the second trade-off parameter C' is selected using Eqs. (5) to theoretically guarantee the ideal convergence rate $O(\frac{1}{T})$ of our GKM.

6.1.3 Unlabeled Data Proportion Analysis

In this simulation study, we address the question how the variation in percentage of unlabeled data influences the learning performance. We also experiment on the real datasets given in Table 1 with various proportions of unlabeled data varied in the grid $\{50\%, 60\%, 70\%, 80\%, 90\%\}$. We observe that when the percentage of unlabeled data increases, the classification accuracy and the F1 score tend to decrease across the datasets except for two datasets COIL20 and MUSHROOMS which remain fairly stable (cf. Table 4 and Figure 3 (left and right)). This observation is reasonable since when increasing the percentage of hidden label, we decrease the amount of information label provided to the classifier, hence making the label propagation more challenging.

6.2 Experimental Results on The Benchmark Datasets

In this experiment, we compare our proposed method with LapSVM, CCCP, Self-KNN and SVM as described in Section 6. Based on the best performance from the empirical model analysis in Section 6.1.2, we use the combination of *Hinge loss* and the *smoothness function* $l_1(\cdot)$ for our model. Besides offering the best predictive performance, this combination also encourages the sparsity in the output solution.

The RBF kernel, given by $K(x, x') = \exp(-\gamma \|x - x'\|^2) = \exp(-\frac{1}{2\sigma_\gamma^2} \|x - x'\|^2)$, is used in the experiments. With LapSVM, we use the parameter settings proposed in [Melacci and Belkin, 2011], wherein the parameters γ_A and γ_l are searched in the grid $\{10^{-6}, 10^{-4}, 10^{-2}, 10^{-1}, 1, 10, 100\}$. In all experiments with the LapSVM, we make use of the preconditioned conjugate gradient version, which seems more suitable for the LapSVM optimization problem [Melacci and Belkin, 2011]. With CCCP-TSVM, we use the setting $\text{CCCP-TSVM}|_{UC^*=LC}^{\gamma=0}$. Only two parameters need to be tuned are the trade-off C and the width of kernel γ . Akin to our proposed GKM, the trade-off parameters $C' = C$ is tuned in the grid $\{2^{-5}, 2^{-3}, \dots, 2^3, 2^5\}$ and the width of kernel γ is varied in the grid $\{2^{-5}, 2^{-3}, \dots, 2^3, 2^5\}$. In our proposed GKM, the bandwidth σ_s of Gaussian kernel weight function, which involves in computing the weights of the spectral graph, is set to $\sigma_s = \sigma_l$. We split the experimental datasets to 90% for training set and 10% for testing set and run cross-validation with 5 folds. The optimal parameter set is selected according to the highest classification accuracy. We set the number of iterations T in GKM to $0.2 \times (l + u)$ for the large-scale datasets such as MUSHROOMS, W5A, W8A, COD-RNA, COVTYPE and IJCNN1 and to $l + u$ for the remaining datasets. Each experiment is carried out five times to compute the average of the reported measures.

We measure the accuracy, training time, and memory amount used in training when the percentages of unlabeled data are 80% and 90%. These measures are reported in Table 5. To improve the readability, in these two tables we emphasize the best method (not count the full-labeled SVM) for each measure using boldface, italicizing, or underlining. Regarding the classification accuracy, it can be seen that GKM are comparable with LapSVM and CCCP while being much better than Self-KNN. Particularly, CCCP seems to be the best method on 80% unlabeled dataset while GKM slightly outperforms others on 90% unlabeled dataset. Comparing with the full-labeled SVM, except for three datasets IJCNN1, COD-RN, and COVTYPE, GKM produces the comparable classification accuracies. Remarkably for the computational time, GKM outperforms the baselines by a wide margin especially on the large-scale datasets. On the large-scale datasets W8A, COD-RNA, IJCNN1, and COVTYPE, GKM is significantly tens of times faster than LapSVM, the second fastest method. We also examine the memory consumption in training for each method. It can be observed that GKM is also economic in terms of memory amount used in training especially on the large-scale datasets. Our GKM consistently uses the least amount of memory in comparison to other methods especially on the large-scale datasets. In contrast, LapSVM always consumes a huge amount of memory during its training. In summary, our GKM is promising to be used in real-world applications since it is scalable, accurate, and economic in memory usage. Most importantly, GKM is the first online learning method for kernelized semi-supervised learning.

7 Conclusion

In this paper, we present a novel framework for semi-supervised learning, called Graph-based Semi-supervised Kernel Machine (GKM). Our framework conjoins three domains

Dataset	Method	Acc 80%	Acc 90%	Time 80%	Time 90%	Memory
G50C	GKM	95.45	96.36	0.015	0.015	2.2
	LapSVM	96.20	94.50	0.29	0.019	5.9
	CCCP	98.18	94.55	0.14	0.509	1.6
	Self-KNN	71.99	63.58	6.68	3.104	8.5
	SVM	96.18	96.18	0.11	0.106	2.7
COIL20	GKM	100.00	100.00	0.01	0.005	2.7
	LapSVM	100.00	100.00	0.39	0.016	11
	CCCP	98.10	100.00	1.1	0.366	1.9
	Self-KNN	93.18	98.67	7.97	1.529	3.3
	SVM	100.00	100.00	0.1	0.090	2.9
USPST	GKM	99.17	100.00	0.031	0.031	3.9
	LapSVM	99.20	99.60	0.28	0.038	9.3
	CCCP	99.58	100.00	0.61	2.170	3.6
	Self-KNN	99.82	99.57	35.4	16.69	3.3
	SVM	99.80	99.80	0.49	0.49	5
AUSTRALIAN	GKM	91.30	90.10	0.021	0.026	3.9
	LapSVM	85.90	86.20	0.94	0.032	4
	CCCP	81.88	89.85	0.04	0.031	3.6
	Self-KNN	84.31	83.76	4.97	2.305	11
	SVM	87.64	87.64	0.027	0.027	2.3
A1A	GKM	81.00	83.49	0.073	0.078	3.3
	LapSVM	80.10	81.60	0.2	0.049	3
	CCCP	79.75	82.37	0.95	0.047	0.7
	Self-KNN	77.71	77.63	32.47	30.724	27
	SVM	83.12	83.12	0.34	0.340	15
MUSHROOMS	GKM	99.94	99.96	0.031	0.037	49
	LapSVM	98.80	97.50	5.26	0.334	337
	CCCP	100.00	99.96	28.1	8.820	177
	Self-KNN	82.92	83.97	551	6,626	37
	SVM	100.00	100.00	632	632.36	106
SVMGUIDE3	GKM	80.24	81.05	0.015	0.015	1.5
	LapSVM	75.80	77.90	0.33	0.028	2.9
	CCCP	81.45	83.37	1.42	0.054	0.7
	Self-KNN	88.24	91.28	18.37	19.21	10
	SVM	83.67	83.67	0.23	0.23	6
W5A	GKM	97.69	97.61	0.041	0.052	103
	LapSVM	97.00	97.50	1.18	0.521	811
	CCCP	98.33	97.39	146.28	7.41	251
	Self-KNN	77.50	65.34	1,778	1,001	84
	SVM	98.49	98.49	48.1	48.06	106
W8A	GKM	97.42	98.00	0.073	0.677	110
	LapSVM	97.40	97.32	26.15	9.150	17,550
	CCCP	97.10	97.18	1,380	379.06	277
	Self-KNN	73.87	71.06	38,481	27,502	388
	SVM	98.82	98.82	64.65	64.65	116
COD-RNA	GKM	87.43	87.51	0.995	1.115	110
	LapSVM	85.70	86.10	13.15	11.42	12,652
	CCCP	88.48	89.74	3,900	326.72	279
	Self-KNN	61.43	63.26	31,370	27,568	649
	SVM	92.04	92.04	7,223	7,223	117
IJCNN1	GKM	93.12	92.62	0.672	0.729	111
	LapSVM	95.30	80.90	15.4	8.08	17,015
	CCCP	93.09	93.29	6,718	302.81	274.3
	Self-KNN	92.93	91.97	12,988	12,739	336
	SVM	98.84	98.84	301	301.48	117
COVTYPE	GKM	83.89	85.29	1.42	1.51	119.5
	LapSVM	81.80	80.20	19.8	34.02	69,498
	CCCP	85.91	85.75	5,958	1,275	292
	Self-KNN	64.30	70.02	19,731	47,875	892
	SVM	90.06	90.06	3,535	3,535	130

Table 5 The classification accuracy (%), training time (Time) (second), and used memory (MB of RAM) of the competitive methods when 80% and 90% of data are hidden label.

of kernel method, spectral graph, and stochastic gradient descent. The proposed GKM can be solved directly in the primal form with the ideal convergence rate $O(\frac{1}{T})$ and naturally inherits all strengths of an SGD-based method. We validate and compare GKM with other state-of-the-art methods in semi-supervised learning on several benchmark datasets. The experimental results demonstrate that our proposed GKM offers comparable classification accuracy and is efficient in memory usage whilst achieving a significant speed-up comparing with the state-of-the-art baselines. Moreover, our approach is the first semi-supervised model offering the online setting that is essential in many real-world applications in the era of big data.

A Appendix on Convex Analysis

Proof of Lemma 1

$$\begin{aligned}\bar{\mathbf{w}}_i &= \frac{i-2}{i}\bar{\mathbf{w}}_{i-1} + \frac{2}{i}\mathbf{w}_{i-1} \\ i(i-1)\bar{\mathbf{w}}_i &= (i-1)(i-2)\bar{\mathbf{w}}_{i-1} + 2(i-1)\mathbf{w}_{i-1}\end{aligned}\quad (6)$$

Taking sum Eq. (6) when $i = 2, \dots, t$, we gain

$$\begin{aligned}t(t-1)\bar{\mathbf{w}}_t &= 2\sum_{i=2}^t(i-1)\mathbf{w}_{i-1} = 2\sum_{i=1}^{t-1}i\mathbf{w}_i \\ \bar{\mathbf{w}}_t &= 2t^{-1}(t-1)^{-1}\sum_{i=1}^{t-1}i\mathbf{w}_i\end{aligned}$$

Proof of Lemma 2. We consider three cases as follows

i) In this case, we have $f(M; a, b, p) = aM^{p-1} - M + b = M^{p-1}(a - M^{2-p}) + b$. Since $M = \max\left(1, (a+b)^{\frac{1}{2-p}}\right)$, we have $M^{p-1} \geq 1$ and $M^{2-p} \geq a+b > a$. Hence, we gain

$$f(M; a, b, p) \leq a - M^{2-p} + b \leq 0$$

ii) With $p = 2$ and $a < 1$, we have $M = \frac{b}{1-a} > 0$ and $f(M; p, a, b) = (a-1)M + b = 0$

iii) In this case, we have

$$\begin{aligned}f(M; a, b, p) &= \frac{a}{(p-1)^{\frac{p-1}{p-2}} a^{\frac{p-1}{p-2}}} - \frac{1}{(p-1)^{\frac{1}{p-2}} a^{\frac{1}{p-2}}} + b \\ &= \frac{a\left(\left(ab^{p-2}(p-1)^{p-1}\right)^{\frac{1}{p-2}} - \left((p-2)^{p-2}\right)^{\frac{1}{p-2}}\right)}{(p-1)^{\frac{p-1}{p-2}} a^{\frac{p-1}{p-2}}} \leq 0\end{aligned}$$

Proof of Lemma 3. We prove that $\|\mathbf{w}_t\| \leq M$ for all t by induction. Assume the hypothesis holds with t , we verify it for $t+1$. We start with

$$\begin{aligned}\mathbf{w}_{t+1} &= \mathbf{w}_t - \eta_t g_t = \frac{t-1}{t+1}\mathbf{w}_t - \frac{2C}{t+1}\nabla_{\mathbf{w}} l(\mathbf{w}_t; x_t, y_t) - \frac{2C'\mu_{u,v_t}}{t+1}\nabla_{\mathbf{w}} l_p(\mathbf{w}_t^\top \Phi_{u,v_t}) \\ \|\mathbf{w}_{t+1}\| &\leq \frac{t-1}{t+1}\|\mathbf{w}_t\| + \frac{2C}{t+1}\|\nabla_{\mathbf{w}} l(\mathbf{w}_t; x_t, y_t)\| + \frac{2C'\mu_{u,v_t}}{t+1}\|\nabla_{\mathbf{w}} l_p(\mathbf{w}_t^\top \Phi_{u,v_t})\| \\ &\leq \frac{t-1}{t+1}\|\mathbf{w}_t\| + \frac{2CA}{t+1} + \frac{2C'\mu_{u,v_t}\|\nabla_{\mathbf{w}} l_p(\mathbf{w}_t^\top \Phi_{u,v_t})\|}{t+1} \\ \|\nabla_{\mathbf{w}} l_p(\mathbf{w}_t^\top \Phi_{u,v_t})\| &\leq \left\| p \text{sign}(\mathbf{w}_t^\top \Phi_{u,v_t}) |\mathbf{w}_t^\top \Phi_{u,v_t}|^{p-1} \Phi_{u,v_t} \right\| \\ &\leq 2Rp\|\Phi_{u,v_t}\|^{p-1}\|\mathbf{w}_t\|^{p-1} \leq (2R)^p p \|\mathbf{w}_t\|^{p-1}\end{aligned}$$

where we have $\|\Phi_{u,v_t}\| = \|\Phi(x_{u_t}) - \Phi(x_{v_t})\| \leq 2R$. Therefore, we gain the following inequality

$$\begin{aligned}\|\mathbf{w}_{t+1}\| &\leq \frac{t-1}{t+1}\|\mathbf{w}_t\| + \frac{2CA}{t+1} + \frac{2C'\mu_{u,v_t}(2R)^p p \|\mathbf{w}_t\|^{p-1}}{t+1} \\ &= \frac{t-1}{t+1}\|\mathbf{w}_t\| + \frac{2b}{t+1} + \frac{2a\|\mathbf{w}_t\|^{p-1}}{t+1} \quad (\text{since } \mu_{u,v_t} \leq 1)\end{aligned}$$

where we denote $a = C'(2R)^p p$ and $b = CA$. Recall that we define M as

$$M = \begin{cases} \max\left(1, (a+b)^{\frac{1}{2-p}}\right) & \text{if } p < 2 \\ \frac{b}{1-a} & \text{if } p = 2, a < 1 \\ \left(\frac{1}{(p-1)a}\right)^{\frac{1}{p-2}} & \text{if } p > 2, ab^{p-2} \leq \frac{(p-2)^{p-2}}{(p-1)^{p-1}} \end{cases}$$

Referring to Lemma 2, we have $f(M; p, a, b) \leq 0$ and gain

$$\begin{aligned}\|\mathbf{w}_{t+1}\| &\leq \frac{t-1}{t+1}M + \frac{2b}{t+1} + \frac{2aM^{p-1}}{t+1} \\ &\leq M + \frac{2(aM^{p-1} - M + b)}{t+1} \leq M + \frac{f(M; p, a, b)}{t+1} \leq M\end{aligned}$$

Therefore, the hypothesis holds for $t+1$. It concludes this proof.

Proof of Lemma 4. To bound $\|g_t\|$, we derive as

$$\begin{aligned}\|g_t\| &\leq \|\mathbf{w}_t\| + C \|\nabla_{\mathbf{w}} l(\mathbf{w}_t; x_t, y_t)\| + C' \mu_{u, v_t} \left\| \nabla_{\mathbf{w}} l_p \left(\mathbf{w}_t^\top \Phi_{u, v_t} \right) \right\| \\ &\leq M + CA + C' (2R)^p p M^{p-1} = G\end{aligned}$$

Proof of Theorem 1

$$\|\mathbf{w}_{t+1} - \mathbf{w}^*\|^2 = \|\mathbf{w}_t - \eta_t g_t - \mathbf{w}^*\|^2 = \|\mathbf{w}_t - \mathbf{w}^*\|^2 + \eta_t^2 \|g_t\|^2 - 2\eta_t g_t^\top (\mathbf{w}_t - \mathbf{w}^*)$$

Taking the conditional expectation w.r.t \mathbf{w}_t , we gain

$$\begin{aligned}\mathbb{E} [\|\mathbf{w}_{t+1} - \mathbf{w}^*\|^2] &= \mathbb{E} [\|\mathbf{w}_t - \mathbf{w}^*\|^2] + \eta_t^2 \mathbb{E} [\|g_t\|^2] - 2\eta_t \mathbb{E} [g_t^\top (\mathbf{w}_t - \mathbf{w}^*)] \\ &= \mathbb{E} [\|\mathbf{w}_t - \mathbf{w}^*\|^2] + \eta_t^2 \mathbb{E} [\|g_t\|^2] + 2\eta_t (\mathbf{w}^* - \mathbf{w}_t)^\top \nabla_{\mathbf{w}} \mathcal{J}(\mathbf{w}_t) \\ &\leq \mathbb{E} [\|\mathbf{w}_t - \mathbf{w}^*\|^2] + \eta_t^2 \mathbb{E} [\|g_t\|^2] + 2\eta_t \left(\mathcal{J}(\mathbf{w}^*) - \mathcal{J}(\mathbf{w}_t) - \frac{1}{2} \|\mathbf{w}_t - \mathbf{w}^*\|^2 \right)\end{aligned}$$

Taking expectation of the above equation again, we yield

$$\begin{aligned}\mathbb{E} [\|\mathbf{w}_{t+1} - \mathbf{w}^*\|^2] &\leq \mathbb{E} [\|\mathbf{w}_t - \mathbf{w}^*\|^2] + \eta_t^2 \mathbb{E} [\|g_t\|^2] \\ &\quad + 2\eta_t \left(\mathcal{J}(\mathbf{w}^*) - \mathbb{E} [\mathcal{J}(\mathbf{w}_t)] - \frac{1}{2} \mathbb{E} [\|\mathbf{w}_t - \mathbf{w}^*\|^2] \right) \\ &\leq (1 - \eta_t) \mathbb{E} [\|\mathbf{w}_t - \mathbf{w}^*\|^2] + G^2 \eta_t^2 + 2\eta_t (\mathcal{J}(\mathbf{w}^*) - \mathbb{E} [\mathcal{J}(\mathbf{w}_t)]) \\ \mathbb{E} [\mathcal{J}(\mathbf{w}_t)] - \mathcal{J}(\mathbf{w}^*) &\leq \left(\frac{1}{2\eta_t} - \frac{1}{2} \right) \mathbb{E} [\|\mathbf{w}_t - \mathbf{w}^*\|^2] - \frac{1}{2\eta_t} \mathbb{E} [\|\mathbf{w}_{t+1} - \mathbf{w}^*\|^2] + \frac{G^2 \eta_t}{2}\end{aligned}$$

Using the learning rate $\eta_t = \frac{2}{t+1}$, we gain

$$\mathbb{E} [t \mathcal{J}(\mathbf{w}_t)] - t \mathcal{J}(\mathbf{w}^*) \leq \frac{(t-1)t}{4} \mathbb{E} [\|\mathbf{w}_t - \mathbf{w}^*\|^2] - \frac{t(t+1)}{4} \mathbb{E} [\|\mathbf{w}_{t+1} - \mathbf{w}^*\|^2] + \frac{G^2 t}{t+1}$$

Taking sum when t runs from 1 to T , we achieve

$$\begin{aligned}\mathbb{E} \left[\sum_{t=1}^T t \mathcal{J}(\mathbf{w}_t) \right] - \frac{T(T+1)}{2} \mathcal{J}(\mathbf{w}^*) &\leq -\frac{T(T+1)}{4} \mathbb{E} [\|\mathbf{w}_{T+1} - \mathbf{w}^*\|^2] + \sum_{t=1}^T \frac{G^2 t}{t+1} < G^2 T \\ \mathbb{E} \left[\frac{2}{T(T+1)} \sum_{t=1}^T t \mathcal{J}(\mathbf{w}_t) \right] - \mathcal{J}(\mathbf{w}^*) &< \frac{2G^2}{T} \\ \mathbb{E} \left[\mathcal{J} \left(\frac{2}{T(T+1)} \sum_{t=1}^T t \mathbf{w}_t \right) \right] - \mathcal{J}(\mathbf{w}^*) &< \frac{2G^2}{T} \\ \mathbb{E} [\mathcal{J}(\bar{\mathbf{w}}_{T+1}) - \mathcal{J}(\mathbf{w}^*)] &< \frac{2G^2}{T}\end{aligned}$$

Furthermore, from the strong convexity of $\mathcal{J}(\cdot)$ and \mathbf{w}^* is a minimizer, we have

$$\begin{aligned}\mathcal{J}(\bar{\mathbf{w}}_{T+1}) - \mathcal{J}(\mathbf{w}^*) + \frac{1}{2} \|\bar{\mathbf{w}}_{T+1} - \mathbf{w}^*\|^2 &\geq \nabla_{\mathbf{w}} \mathcal{J}(\mathbf{w}^*)^\top (\bar{\mathbf{w}}_{T+1} - \mathbf{w}^*) \geq \frac{1}{2} \|\bar{\mathbf{w}}_{T+1} - \mathbf{w}^*\|^2 \\ \mathbb{E} [\|\bar{\mathbf{w}}_{T+1} - \mathbf{w}^*\|^2] &< \frac{4G^2}{T}\end{aligned}$$

Proof of Theorem 2. Let us denote the random variable $Z_{T+1} = \mathcal{J}(\bar{\mathbf{w}}_{T+1}) - \mathcal{J}(\mathbf{w}^*) \geq 0$. From Markov inequality, we have

$$\begin{aligned}\mathbb{P}[Z_{T+1} \geq \varepsilon] &\leq \frac{\mathbb{E}[Z_{T+1}]}{\varepsilon} = \frac{\mathbb{E}[\mathcal{J}(\bar{\mathbf{w}}_{T+1}) - \mathcal{J}(\mathbf{w}^*)]}{\varepsilon} < \frac{2G^2}{T\varepsilon} \\ \mathbb{P}[Z_{T+1} < \varepsilon] &> 1 - \frac{2G^2}{T\varepsilon}\end{aligned}$$

By choosing $T_0 = \left\lceil \frac{2G^2}{\varepsilon\delta} \right\rceil$, for all $T \geq T_0$, we have $\mathbb{P}[Z_{T+1} < \varepsilon] > 1 - \frac{2G^2}{T\varepsilon} \geq 1 - \delta$.

References

- A. Azran. The rendezvous algorithm: Multiclass semi-supervised learning with markov random walks. In *Proceedings of the 24th International Conference on Machine Learning, ICML '07*, pages 49–56, 2007.
- M. Belkin, P. Niyogi, and V. Sindhwani. Manifold regularization: A geometric framework for learning from labeled and unlabeled examples. *J. Mach. Learn. Res.*, 7:2399–2434, December 2006.
- A. Blum and S. Chawla. Learning from labeled and unlabeled data using graph mincuts. In *Proceedings of the Eighteenth International Conference on Machine Learning, ICML '01*, pages 19–26, 2001.
- A. Blum, J. D. Lafferty, M. R. Rwebangira, and R. Reddy. Semi-supervised learning using randomized mincuts. In *ICML*, volume 69, 2004.
- C.-C. Chang and C.-J. Lin. Libsvm: A library for support vector machines. *ACM Trans. Intell. Syst. Technol.*, 2(3):27:1–27:27, May 2011. ISSN 2157-6904.
- O. Chapelle and A. Zien. Semi-supervised classification by low density separation, 2005.
- O. Chapelle, J. Weston, and B. Schölkopf. Cluster kernels for semi-supervised learning. In *Advances in Neural Information Processing Systems 15*, pages 601–608. MIT Press, 2003.
- O. Chapelle, M. Chi, and A. Zien. A continuation method for semi-supervised svms. In *Proceedings of the 23rd international conference on Machine learning*, pages 185–192, 2006.
- O. Chapelle, V. Sindhwani, and S.S. Keerthi. Optimization techniques for semi-supervised support vector machines. *Journal of Machine Learning Research*, 9:203–233, June 2008.
- R. Collobert, F. Sinz, J. Weston, L. Bottou, and T. Joachims. Large scale transductive svms. *Journal of Machine Learning Research*, 2006.
- C. Cortes and V. Vapnik. Support-vector networks. In *Machine Learning*, pages 273–297, 1995.
- T. De Bie and N. Cristianini. Semi-supervised learning using semi-definite programming. In *Semi-supervised Learning*, Cambridge, MA, 2006.
- P. Duong, V. Nguyen, M. Dinh, T. Le, D. Tran, and W. Ma. Graph-based semi-supervised support vector data description for novelty detection. In *2015 International Joint Conference on Neural Networks (IJCNN)*, pages 1–6, July 2015.
- G. Getz, N. Shental, and E. Domany. Semi-supervised learning – a statistical physics approach. *CoRR*, 2006.
- C. Goutte, H. Déjean, E. Gaussier, N. Cancedda, and J-M Renders. Combining labelled and unlabelled data: A case study on fisher kernels and transductive inference for biological entity recognition. In *Proceedings of the 6th Conference on Natural Language Learning - Volume 20, COLING-02*, pages 1–7, 2002.
- T. Joachims. Transductive inference for text classification using support vector machines. In *International Conference on Machine Learning (ICML)*, pages 200–209, 1999.
- T. Joachims. Transductive learning via spectral graph partitioning. In *In ICML*, pages 290–297, 2003.
- S. Kakade and Shalev-Shwartz. Mind the duality gap: Logarithmic regret algorithms for online optimization. In *NIPS*, 2008.
- N. Kasabov, D. Zhang, and P.S. Pang. Incremental learning in autonomous systems: evolving connectionist systems for on-line image and speech recognition. In *Advanced Robotics and its Social Impacts, 2005. IEEE Workshop on*, pages 120 – 125, june 2005.
- R. I. Kondor and J. D. Lafferty. Diffusion kernels on graphs and other discrete input spaces. pages 315–322. Morgan Kaufmann Publishers Inc., 2002. ISBN 1-55860-873-7.
- S. Lacoste-Julien, M. W. Schmidt, and F. Bach. A simpler approach to obtaining an $o(1/t)$ convergence rate for the projected stochastic subgradient method. *CoRR*, 2012.
- T. Le, D. Tran, T. Tran, K. Nguyen, and W. Ma. Fuzzy entropy semi-supervised support vector data description. In *International Joint Conference on Neural Networks (IJCNN)*, pages 1–5, Aug 2013.
- Trung Le, Phuong Duong, Mi Dinh, Tu Dinh Nguyen, Vu Nguyen, and Dinh Phung. Budgeted semi-supervised support vector machine. In *The 32th Conference on Uncertainty in Artificial Intelligence*, pages 377–386. AUAI Press, 2016.
- Y-F. Li and Z-H. Zhou. Towards making unlabeled data never hurt. *Pattern Analysis and Machine Intelligence, IEEE Transactions on*, 37(1):175–188, Jan 2015.
- S. Melacci and M. Belkin. Laplacian support vector machines trained in the primal. *J. Mach. Learn. Res.*, 12:1149–1184, July 2011.
- V. Nguyen, T. Le, T. Pham, M. Dinh, and T. H. Le. Kernel-based semi-supervised learning for novelty detection. In *International Joint Conference on Neural Networks (IJCNN)*, pages 4129–4136, July 2014.
- S. Shalev-shwartz and Y. Singer. Logarithmic regret algorithms for strongly convex repeated games. In *The Hebrew University*, 2007.
- S. Shalev-Shwartz and T. Zhang. Stochastic dual coordinate ascent methods for regularized loss. *Journal of Machine Learning Research*, 14(1):567–599, 2013.
- V. Sindhwani and P. Niyogi. Linear manifold regularization for large scale semi-supervised learning. In *Proc. of the 22nd ICML Workshop on Learning with Partially Classified Training Data*, 2005.

- V. Sindhwani, S.S. Keerthi, and O. Chapelle. Deterministic annealing for semi-supervised kernel machines. In *Proceedings of the 23rd international conference on Machine learning, ICML '06*, pages 841–848, 2006.
- A. J. Smola and I. R. Kondor. Kernels and regularization on graphs. In *Proceedings of the Annual Conference on Computational Learning Theory*, 2003.
- J. Tan, L. Zhen, N. Deng, and Z. Zhang. Laplacian p-norm proximal support vector machine for semi-supervised classification. *Neurocomputing*, 144:151–158, 2014.
- I. W. Tsang and J. T. Kwok. Large-scale sparsified manifold regularization. pages 1401–1408. MIT Press, 2006. ISBN 0-262-19568-2.
- L. Wang, K. L. Chan, and Z. Zhang. Bootstrapping svm active learning by incorporating unlabelled images for image retrieval. pages 629–634. IEEE Computer Society, 2003.
- Y. Wang, S. Chen, H. Xue, and Z. Fu. Semi-supervised classification learning by discrimination-aware manifold regularization. *Neurocomputing*, 147:299–306, 2015.
- F. Wu, W. Wang, Y. Yang, Y. Zhuang, and F. Nie. Classification by semi-supervised discriminative regularization. *Neurocomputing*, 73:1641 – 1651, 2010. ISSN 0925-2312.
- X. Zhu and Z. Ghahramani. Towards semi-supervised classification with markov random fields, 2002.
- X. Zhu, Z. Ghahramani, and J. D. Lafferty. Semi-supervised learning using gaussian fields and harmonic functions. In *IN ICML*, pages 912–919, 2003.
- X. Zhu, A. B. Goldberg, R. Brachman, and T. Dietterich. *Introduction to Semi-Supervised Learning*. Morgan and Claypool Publishers, 2009. ISBN 1598295470, 9781598295474.